Thermal Characterization of Molten Salt Battery Materials

Stephen L. Hodson[1,2], Edward S. Piekos[1], Robert A. Sayer[1], Scott A. Roberts[1], Christine C. Roberts[1]

[1]Engineering Sciences Department
Sandia National Laboratory
PO Box 5800, Albuquerque, New Mexico, 87185

[2]Purdue University
School of Mechanical Engineering
610 Purdue Mall, West Lafayette, IN 47907

Abstract: *Molten salt batteries are particularly useful power sources for radar and guidance systems in military applications such as guided missiles, ordinance, and other weapons. Molten salt batteries are activated by raising the temperature of the electrolyte above its melting temperature using pyrotechnic heat pellets. The battery will remain active as long as the electrolyte is molten. As a result, the thermal processes within the components and interactions between them are critical to the overall performance of molten salt batteries. A molten salt battery is typically thermally insulated using wrappable and board-like insulation materials such as Fiberfrax wrap, Fiberfrax board, and Min-K insulation. The Fiberfrax board and Min-K insulation are composites of alumino-silicate and fumed silica-titania, respectively. In this work, the thermal conductivities of the Fiberfrax board and Min-K insulation are measured under different uniaxial compressive states and ambient environments. The thermal conductivity of the mixed separator pellets (LiCl/MgO/KCl) was also measured along with its contact resistances with interfacing members. To measure the thermal quantities, a steady-state reference bar with thermocouples was employed. The resulting values serve as inputs to a thermal model that aims to predict lifetimes of the batteries. Improvements to a thermal model for an example battery due to the revised thermal property values are discussed.*

Keywords: Thermal batteries; thermal conductivity; separator; Min-K; Fiberfrax; insulation; 1D reference-bar

Introduction

The overall performance of molten salt batteries is dictated by complex multiphysics consisting of electrochemical processes, mechanical responses, and thermal transport mechanisms. The molten electrolyte and separator [LiCl/KCl, MgO] serve as the battery's hub by providing an ionically conductive path between the anode [Li(Si)] and cathode [$CaCrO_4$ or FeS_2]. Depending on the application, the desired lifetimes can vary between a few seconds and one hour [1], which is partially dictated by the cooling rate of the molten electrolyte. To mitigate cooling, molten salt batteries are packaged with insulation materials such as Fiberfrax board and Min-K thermal insulation. The latter is often employed in molten salt batteries that require long lifetimes [2]. These insulations are included at the top and bottom of the battery stack and are compressed under force before the battery can is sealed. Other Fiberfrax insulation is wrapped around the stack under tension.

Predictive models for molten salt battery activation can be improved with high fidelity measurements of thermal properties such as heat capacity and thermal conductivity. Specifically, non-molten separator thermal conductivity is necessary for predicting rise time whereas insulation thermal conductivity has been found to be a great source of uncertainty in predicting the lifetime of the battery [2]. Currently, the insulation thermal conductivity is not implemented as a function of strain in the Sandia multiphysics model for battery activation (TABS v 3.0).

Various techniques, either steady state or transient, can be employed to measure thermal conductivities of materials and each has advantages and disadvantages. Transient techniques such as laser flash, thermoreflectance, and photoacoustic provide quick determination of thermal conductivities relative to steady state techniques, but generally require prior knowledge of the density and heat capacity of the material. Steady state techniques such as reference bar and infrared thermography do not require knowledge of the density and heat capacity, but are not suitable for rapid characterization of large quantities of samples. In this work, a steady state technique [4] was used to measure the thermal conductivities of the separator pellets as well as annealed Fiberfrax board and Min-K insulation materials in different ambient environments and compressive stresses which are congruent with common molten salt battery packaging protocols.

Experimental Setup

The separator material was formed by mixing, melting, and grinding LiCl/KCl electrolyte salt with MgO to form a powder. The mixture was then hydraulically pressed to form LiCl/MgO/KCl pellets of varying thicknesses. Pellets were all 1.75 g/cm^3 in density.

The Fiberfrax board and Min-K insulation materials were purchased in a variety of thicknesses from Unifrax and Morgan Thermal Ceramics, respectively. The insulation materials were then annealed in dry air at 600°C for 4 hours to remove moisture and stored in a dry environment until tested. SEM images showing the cross-section of the insulation materials are shown below in Figures 1(a) and (b).

The steady state reference bar technique is based on the ASTM D470-06 standard for measuring thermal conductivity and contact resistance and is used to measure the thermal conductivity of the different materials as well as the contact resistance with stainless steel 304 (SS304)

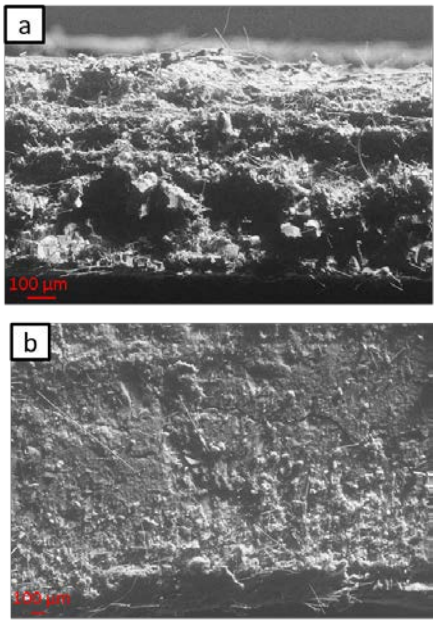

Figure 1. Cross-sectional SEM images of (a) annealed Fiberfrax board and (b) annealed Min-K.

and Macor heat flux meters. The system, shown in Figure 2 uses thermocouples to measure the temperature gradient in the heat flux meters while a mechanical translator compresses the interface to a load which is measured by a load cell. The mechanical translators are terminated with flat plates which are also cooled and heated to constant temperatures. The system has the capability to measure thermal properties in Ar, He, N_2, air, and vacuum, which can simulate the hermitically sealed environment of the battery and gases released during chemical reactions. Note that thermal conductivity values measured by this technique are solely in the cross-plane direction.

When compressed to a constant strain, Fiberfrax and Min-K insulations are known to undergo stress relaxation for extended periods of time. Therefore, both load and strain were measured simultaneously during measurements. Strain was recorded using a camera image of the sample.

The thermal model that accompanies the measurement technique is based on the one dimensional heat conduction equation and depending on the ambient environment (vacuum or gas), includes radiative and convective losses to the surroundings. The temperature throughout the stack is determined by solving Eq. 1 below:

$$\frac{d}{dx}\left(k_{HFM}\frac{dT}{dx}\right)-\varepsilon\sigma\left(T^4-T_{surr}^4\right)-h\left(T-T_\infty\right)=0 \qquad \text{Eq. 1}$$

where T is the temperature in the stack along the direction x, k_{HFM} is the thermal conductivity of the heat flux meter, ε is the emissivity of the heat flux meter, σ is the Stefan-Boltzmann constant, T_{surr} is the temperature of the surroundings that exchange thermal radiation with the heat flux meters, h is the convective heat transfer coefficient and T_∞ is the average temperature of the ambient gas. The total thermal resistance between the top and bottom heat flux meters is determined by fitting Eq. 1 to the temperature profiles in the heat flux meters using COMSOL. For the separator pellets, SS304 heat flux meters were chosen while Macor heat flux meters were chosen for the insulation materials. Note that the thermal conductivity of the Macor heat flux meters was determined by testing the material against SS304 bars of known thermal conductivity. The temperature profile and the thermal conductivity of the heat flux meters are used to determine the heat flux, temperature drop, and ultimately the thermal resistance across the interface. In Eq. 2 below, the total thermal resistance between the heat flux meters (R_{total}) comprises of two contact resistances (R_{TCR}) that are in series with the bulk (intrinsic) resistance (R_{bulk}) of the material of interest:

$$R_{total}=R_{bulk}+R_{TCR}=\frac{t}{k}+R_{TCR} \qquad \text{Eq. 2}$$

where t and k are the thickness and thermal conductivity of the material of interest, respectively. The thermal conductivity can be determined by measuring the total thermal resistance between the heat flux meters for different thicknesses of the material of interest. This produces a linear relationship between thermal resistance and material thickness in which the inverse slope of the linear relationship is the thermal conductivity and the y-intercept is the contact resistance. The uncertainties associated with this measurement technique include thermocouple error, uncertainty in estimating the thickness, regression uncertainty, and sample to sample uncertainty.

Results and Discussion

Thermal conductivity measurements on the separator pellets (LiCl/MgO/KCl) were conducted within the pressure range of 400 and 2250 kPa and an average interface temperature (material temperature) of approximately 45°C. Due to the fact that the molten salt battery materials are moisture sensitive, the system was purged with dry air (5-10% humidity) during thermal testing. Tests were conducted on mixtures of three distinct thicknesses of 0.5, 1, and 2 mm. The thermal conductivity of the mixture and contact resistance with the heat flux meters were estimated by a linear fit to the measured thermal resistance and mixture thicknesses for interface pressures of 400, 1700, and 2250 kPa.

The variation in the measured thermal resistance for samples of the same thickness is greatest at lower interface pressures and smallest at the highest interface pressure. This indicates that the sample to sample uncertainty decreases with increasing pressure and that the misalignment between the separator pellet and heat flux meters is mitigated as the pressure increases. The thermal conductivity and contact resistance as functions of interface pressure are shown below in Figure 3(a) and (b), respectively. The error bars include the sample to sample, linear fit, and thermocouple uncertainty.

The thermal conductivity of the separator pellets remains constant with interface pressure with a mean value of 2.30 W/mK with a lower and upper bound of 2.08 and 2.49 W/mK, respectively, at an interface pressure of 2250 kPa. As expected, the contact resistance of the separator pellets with the heat flux meters monotonically decreases with interface. Therefore, the separator pellets are not being affected by the compressive stress that is applied during the measurement, except that the contact with the instrument bars improves.

Thermal conductivity measurements on the Min-K and Fiberfrax board insulation materials were conducted at compressive stresses of 350 and 500 psi with an average material temperature of approximately 55°C. To assess the thermal transport mechanisms across the insulation materials, the samples were tested in both air and vacuum ambient environments. The test sequence was as follows: (i) air at 350 psi, (ii) vacuum at 350 psi, (iii) vacuum at 500 psi, and (iv) air at 500 psi. Figures 4(a)-(d) below shows the linear fits to the measured thermal resistances in air and insulation thicknesses for the aforementioned test sequence. Vacuum data was also obtained but is not shown. The error bars include errors due to thermocouple readings and estimation in material thickness. With coefficients of determination ranging between 0.86 and 0.99 for the experimental data presented in Figure 4, a linear fit properly describes the change in thermal resistance with material thickness. As such, the thermal conductivity of each material can be determined by the inverse slope of the linear fit. The thermal conductivity values for both insulation materials are summarized in Table 1 below and are in good agreement with the work of Guidotti et al. [2]. Note that the contact resistances between the insulation and Macor heat flux meters are not shown because the intrinsic (bulk) resistance of the insulations dominates thermal transport.

The changes in thermal conductivity with respect to the ambient environment and compression are consistent between the Min-K and Fiberfrax board insulations. When the test chamber is evacuated, the thermal conductivities decrease by 25% and 43%, respectively. Upon compression to 500 psi in vacuum, the thermal conductivities increase by 19% and 16%, respectively. When air is subsequently introduced into the test chamber to atmospheric pressure, the thermal conductivities increase by 50% and 78%. Comparing the thermal conductivities in air at 350 and 500 psi shows that compression of the insulations in air results in an increase in thermal conductivity of 25% and 19%, respectively.

The changes in thermal conductivity of the insulation materials suggest that the ambient environment and compressive stress serve significant roles in thermal transport throughout the insulation materials. Depending

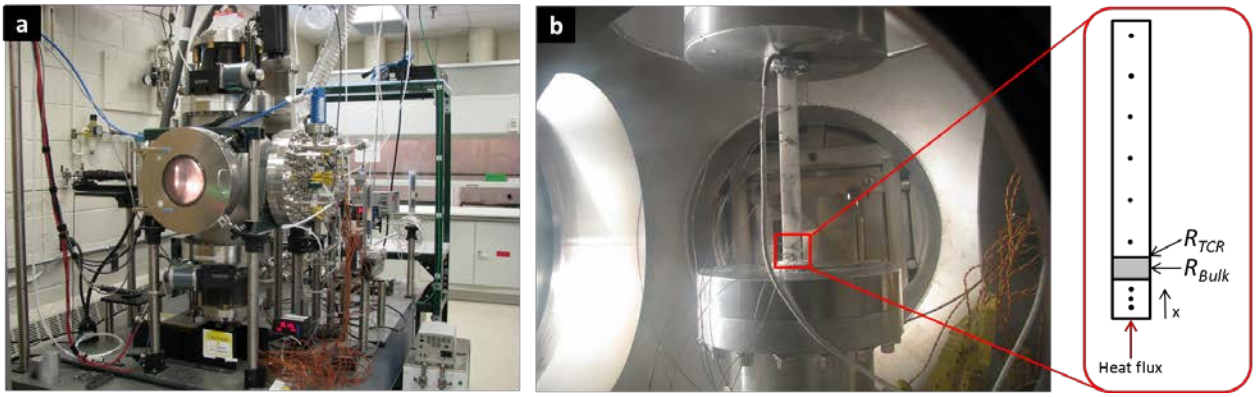

Figure 2. Thermal conductivity measurement system utilizing a 1D reference bar technique. Photographs of (a) the vacuum chamber and (b) the heat flux meters (HFMs) instrumented with thermocouples.

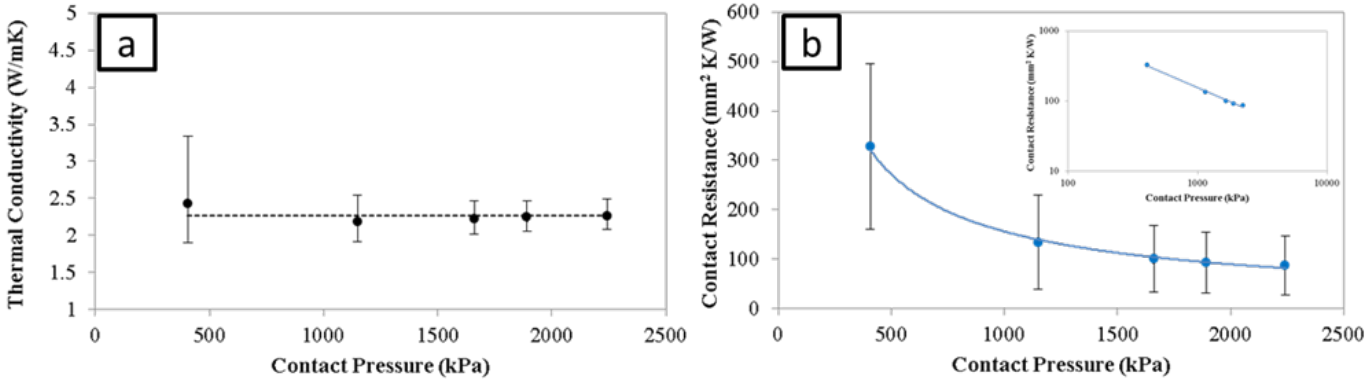

Figure 3. (a) Separator thermal conductivity and (b) Separator-heat flux meter contact resistance as a function of contact pressure. Inset: Contact resistance vs. pressure on a log-log scale

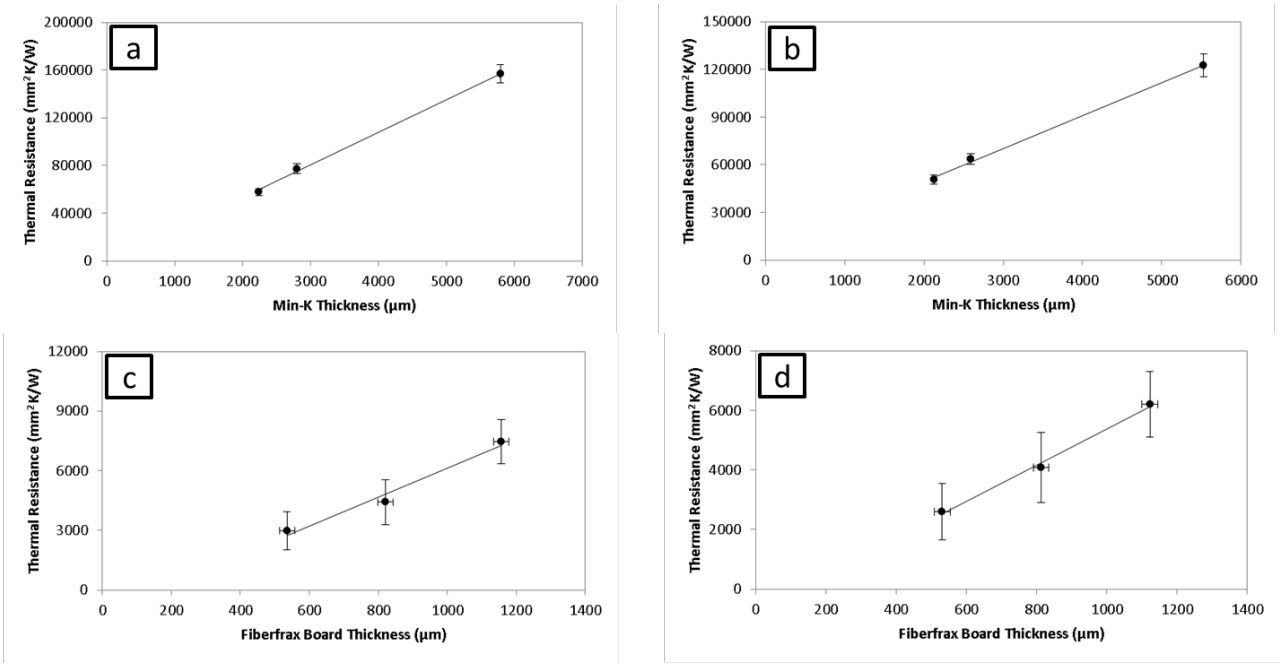

Figure 4. Thermal resistance in air as a function of insulation thickness for (a) Min-K at 350 psi, (b) Min-K at 500 psi (c) Fiberfrax board at 350 psi and (d) Fiberfrax board at 500 psi.

on the porosity of the insulation materials, thermal transport through the air medium can serve as a parallel pathway for heat transfer. In this sense, the thermal conductivity of the insulation materials is an effective thermal conductivity that comprises of thermal transport through the alumino-silicate (Fiberfrax board) or fumed silica-titania (Min-K) as well as the air medium. In the absence of the latter, thermal transport is relegated only through the solid medium. The granular and fibrous microstructure as observed in the cross-sectional SEM images in Figures 1 suggest that upon compression, the insulation materials densify and larger microscopic contact regions between the constituent particles of the insulation materials are formed, which ultimately increases the thermal conductivity.

Table 1. Thermal conductivity (W/mK) of Fiberfrax board and Min-K insulations under different conditions

k (W/mK)	**Min-K**		**Fiberfrax**	
Compressive stress (psi)	Air	Vacuum	Air	Vacuum
350	0.036	0.027	0.138	0.079
500	0.048	0.032	0.164	0.092

Conclusions

A steady state reference bar technique was employed to measure the thermal conductivities of the separator pellets (LiCl/MgO/KCl) and thermally insulating materials (Fiberfrax board and Min-K). The separator thermal conductivity was measured to be approximately 2.30 W/mK and constant within the pressure range of 400 and 2250 kPa. The effective thermal conductivity of the Fiberfrax board and Min-K insulation materials were measured to be on the order of O(0.1) W/mK and O(0.01) W/mK, respectively, at 350 and 500 psi. The thermal conductivities exhibited dependence on both the ambient environment and compressive stress.

Acknowledgements

Sandia National Laboratories is a multi-program laboratory managed and operated by Sandia Corporation, a wholly owned subsidiary of Lockheed Martin Corporation, for the U.S. Department of Energy's National Nuclear Security Administration under contract DE-AC04-94AL85000.

References

1. R. A. Guidotti, F. W. Reinhardt, and T. Kaun. "Characterization of Small Vac. Multifoil Containers for a One-Hour Thermal Batt.," *Proceedings of the 40th Power Sources Conference*, pp. 299, 2002.
2. Trembacki, B. L. et al. "Uncertainty Quantification, Verification, and Validation of a Thermal Simulation Tool for Molten Salt Batteries", *Proceedings of the 47th Power Sources Conference*, 2016.
3. R. A. Guidotti and M. Moss. "Thermal Conductivity of Thermal-Batt. Insulations," Technical Report SAND 95-1649, Sandia National Laboratories, August 1995.
4. "Standard Test Meth. for Thermal Trans. Prop. of Thermally Conductive Elect. Insulation Mat.," Annu. B. ASTM Stand., pp. D5470–06, 2011.